# Characterization of a hybrid catalytic radiant burner fuelled with methane – hydrogen mixtures

by C. Allouis*, S. Cimino*, R. Nigro**

\* Istituto Ricerche sulla Combustione – CNR – P.le V. Tecchio 80, 80125, Napoli – Italy, _allouis@irc.cnr.it_
\*\*DICMAPI Univ. Napoli Federico II – P.le V. Tecchio 80, 80125, Napoli – Italy, _rnigro@unina.it_

## Abstract

The novel concept of hybrid catalytic combustion based on Catalytic Partial Oxidation + homogeneous flame combustion was tested for the first time with fuel mixtures of methane and hydrogen. CPO experiments were run to elucidate the effect of the progressive substitution of $CH_4$ with $H_2$ in the fuel feed. Furthermore a prototype radiant hybrid burner was safely operated and characterized with up to 80% vol. of $H_2$ in the fuel and a primary equivalence ratio in the range 2.4 – 4.0. Outstanding $NO_x$ emission levels were attained due to the effective reduction of both thermal and prompt $NO_x$ formation.

## 1. Introduction

An increasing concern regarding environmental pollution during the last years has resulted in stricter emission regulations for $NO_x$, CO and greenhouse gases form combustion processes. Lean-premixed combustion technology which has demonstrated the ability to achieve an impressive reduction in $NO_x$ emissions during operation on natural gas [1] industrial and utility gas turbine non-adiabatic burners for domestic and industrial applications.The advent of $H_2$ as a potential alternative for fossil fuel, and increasing availability of hydrogen-containing fuels, i.e. from biomass/coal conversion processes, have generated interest in the possible use of hydrogen-hydrocarbon blends in combustion devices [2]. As a result of the high flame speed and the wide flammability limits of $H_2$, flashback is an issue with lean premixed combustion. Therefore, diffusion flame combustion is typically employed resulting in high levels of $NO_x$ emissions unless steam or nitrogen are added as diluents or exhaust gas cleanup is implemented [3]. This is not economically feasible for small scale domestic and industrial Combined Heat and Power applications.The catalytic partial oxidation (CPO) of various fuels has been proposed as a preliminary conversion stage in hybrid burners for gas turbines with ultra low-$NO_x$ emissions [4 and ref. therein]. Recently the concept has been extended to develop a novel class of hybrid catalytic gas burners, with integrated interstage heat removal by IR radiation from the hot structured catalytic partial oxidation reactor/radiator [5,6], showing significant improvements with respect to the state-of-the-art fully premixed or blue-flame diffusive natural gas burners for domestic condensing boilers [5]. Since the air-fuel mixture fed to the burner is generally above its upper flammability limit, this technology is intrinsically safe and can be regarded as a candidate also for hydrogen-hydrocarbon blends, although only a few data are available. Structured CPO catalysts based on noble metals (particularly Rh, Pt) supported onto ceramic and metallic honeycombs, foams or gauzes have shown high syn-gas yields when operated under auto-thermal conditions at very short contact times with hydrocarbon feeds from methane up to diesel and jet-fuels, alcohols and bioderived liquids [4-8].

In this work we set out to demonstrate the intrinsically safe multi-fuel operability of the novel hybrid catalytic burner and its low $NO_x$ emission performance when fuelled with $H_2$-$CH_4$ mixtures of variable compositions (up to 80% vol. of $H_2$).

## 2. Experimental

Bimetallic Rh-Pt catalysts dispersed on commercial La-γ-$Al_2O_3$ (SCFa140-L3 Sasol, 140m$^2$/g) were prepared via sequential impregnations (incipient wetness) using aqueous solutions of Rh $(NO_3)_3$ and $H_2PtCl_6$ to achieve a total PM loading of 0.5+0.5 %wt [9]. The catalytic layer was washcoated and anchored over high temperature structured substrates by a dip-coating procedure [9]. Cordierite honeycomb disks (D=17mm L=10mm, 600cpsi by NGK) with straight and parallel channels of roughly square section were employed for lab-scale CPO tests. For the prototype burner the catalytic element was realized with a metallic gauze made of a FeCrAlloy knitted wire (d≈ 120 μm) in the form of flexible cylindrical sockets (D=80mm, H=80mm, thickness 2mm, apparent density 0.38 g/cm$^2$, Figure 1) [6]. SEM observations of the coated FeCrAlloy gauze (Fig. 1) revealed the presence of a well adhering porous layer on the metallic wire with an average thickness in the range 7-14 μm. A FLIR Phoenix infrared thermocamera with digital acquisition system and spectral sensitivity in the range 1.5-5 μm was employed to characterize the operation of the hybrid burner, obtaining simultaneously the temperature profile on the outer catalytic surface and an estimation of the flame temperature and structure. In particular, two optical spectral filters centred at 3.9 μm and at 4.25 μm were applied respectively in order to eliminate flame (gas) emissivity when measuring the surface temperature of the catalyst, and to estimate $CO_2$ (flame) temperature [10].

## 2.1. Catalytic Partial Oxidation experiments

Catalytic partial oxidation tests were run under self-sustained high temperature conditions at fixed preheating (230°C), using simulated air as the oxidant (P=1.1 bar). Experiments with pure $CH_4$ fuel were run at a feed equivalence ratio for combustion ($\phi$) from 2.8 to 5.2; CPO tests with $CH_4$-$H_2$ mixtures with variable $H_2$ contents ($yH_2$ up to 80% vol. of the fuel) were run at fixed ($\phi$); according to the lower heat of reaction and lower amount of $O_2$ required for the $H_2$ combustion, the fuel-mix flow rate increased when increasing its $H_2$ content (constant input power for each $\phi$), which was partially compensated by a reduction in the air flow. Reactor temperatures were measured by K-type thermocouples placed inside the catalytic honeycomb, as well as in the gas downstream of it. Real time gas analysis was performed for $CH_4$, $CO$, $CO_2$, $H_2$, $O_2$, $NO$, $NO_2$. $O_2$ was completely converted at steady state; $H_2O$ production was calculated from the O-balance. C- and H- balances were closed within $\pm1.5\%$ and $\pm3.0\%$ respectively. Further details on the experimental set-up can be found in [9].

## 2.2. Hybrid catalytic burner testing

The hybrid catalytic burner under typical operation together with a rendering of its longitudinal section are presented in Figure 1: the fresh gas mixture flowed radially through a perforated hollow cylindric distributor, the CPO gauze reactor and then into the flame [5]. The hybrid burner was tested in upward position with secondary air for the purely diffusive flame combustion withdrawn by natural convection. Combustion tests were performed with a feed $\phi$ in the range 2.4 – 4.0 (i.e. above upper flammability limit). The $H_2$ content in the $H_2$-$CH_4$ mix was varied between 0 to 80% vol., at constant nominal power (6.6, 9.6 and 19.2 kW). High-purity gases calibrated via mass-flow controllers, were pre-mixed and fed to the burner without preheating, at a gas hourly space velocity (GHSV) comprised between 0.1 to 1.0 $\times10^6$ $h^{-1}$ referred to the empty volume of the mesh. Exhaust gases were collected by a hood and the emissions of CO, $NO_x$ and $CH_4$ were corrected to 0% $O_2$.
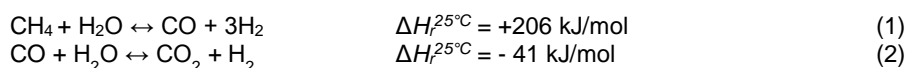
The FLIR Phoenix infrared camera was set-up as a broadband sensor sensitivity in the range 1.5-5 µm to characterize the operation of the hybrid burner, obtaining simultaneously the temperature profile on the outer catalytic surface and an estimation of the flame temperature and structure. In particular, two optical spectral filters centred at 3.9 µm and at 4.25 µm were applied respectively in order to eliminate flame (gas) emissivity when measuring the surface temperature of the catalyst, and to estimate $CO_2$ (flame) temperature [10]. Moreover, the flame images filtered at 3.9 µm allowed us to follow the eventual presence of soot formation. Independent thermocouple measurements were preliminary performed to set appropriate emissivity factors [9]. All the IR pictures presented hereafter represent a 5s-average of the images collected at 340 frames/s. The temperature of the syn-gas emerging from the catalytic stage was also measured with a shielded (Inconel 600, d=0.5mm) K-type thermocouple placed 1 mm downstream from the catalyst surface and parallel to it.
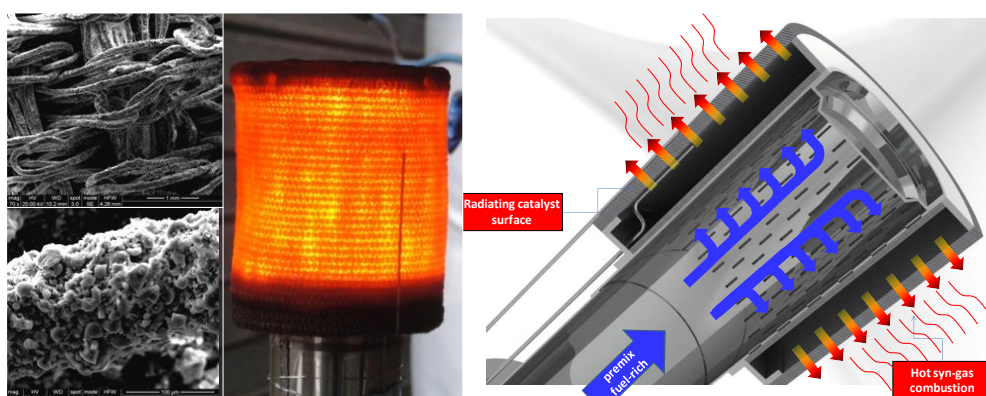


**Fig. 1.** *SEM images at increasing magnifications of the FeCrAlloy knitted gauze substrate with active washcoat layer (left); catalytic combustion head (DxL=80x80 mm) during operation (centre), and rendering of its section (right).*

## 3. Results and Discussion

During the CPO of pure methane over structured catalysts based on Rh and Pt, $O_2$ is rapidly depleted within a short front section of the catalyst bed and a significant portion of fuel is consumed to produce a mixture of $H_2$, $CO$ and $H_2O$ [11-12]. Methane steam reforming (SR, Eq. (1)) is a slower reaction [9, 11-12] prevailing in that remaining part of the reactor after the oxidation zone, where the water-gas-shift ((WGS, Eq. (2)) reaction also proceeds quickly to equilibrium.

$$CH_4 + H_2O \leftrightarrow CO + 3H_2 \qquad \Delta H_r^{25°C} = +206 \text{ kJ/mol} \qquad (1)$$
$$CO + H_2O \leftrightarrow CO_2 + H_2 \qquad \Delta H_r^{25°C} = -41 \text{ kJ/mol} \qquad (2)$$

Due to the limited oxygen availability in the feed, the catalytic performances of the CPO reactor are strictly controlled by the inlet equivalence ratio $\phi$. As shown in Fig. 2 a-b methane conversion and catalyst temperatures decreased monotonically with increasing $\phi$ from 2.8 to 5.2, without affecting stable steady state operation of the CPO reactor, whose outlet temperature ranged from 600°C to 900°C.
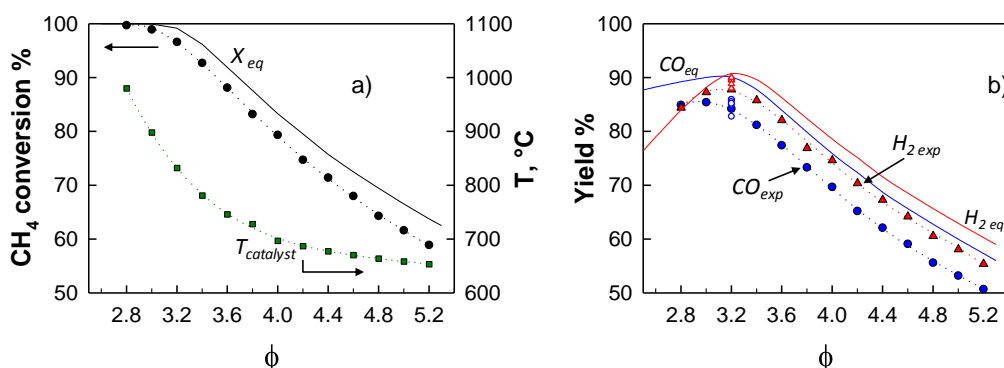


*Fig. 2. Methane conversion, catalyst temperature, and yields to CO and $H_2$ during the CPO of pure $CH_4$ in air over Rh-Pt honeycomb as a function of the equivalence ratio $\phi$. Solid lines represent equilibrium values (p, H=constant).*

Yields to CO and $H_2$ passed through a maximum for $\phi$=3. Experimental curves followed the trends of adiabatic equilibrium calculated excluding solid carbon formation (solid lines in Fig. 2a-b), which was never observed experimentally, and departed from them due to heat losses from the hot catalytic monolith. It should be considered that testing under non-adiabatic conditions is required in view of the use of structured CPO reactors as radiant elements in hybrid catalytic burners [5,6]. In general the thermal efficiency of the lab-scale reactor [12] varied between 0.78 and 0.85. Repeated experiments were performed at $\phi$=3.2 (Fig. 2b) by varying the GHSV by a factor 2.6 (maximum 1.2 $10^5$ h$^{-1}$ based on the volume of the honeycomb catalyst), and showed a small positive effect of increasing flow rates on the yields to CO and $H_2$; that is related to a higher thermal efficiency of the catalytic reactor, which more than compensated for the lower contact time [12].

The effect of increasing the $H_2$ content during the steady state operation of the CPO reactor with methane-hydrogen blends is presented in Figure 3 a-d for two values of the feed equivalence ratios (3.6 and 4.2). The partial substitution of methane with $H_2$ at each fixed value of $\phi$ caused an increase of the temperature of the catalyst and of the product gas, in agreement with the trends of the adiabatic equilibrium temperature (Fig. 3a). This effect is due to the larger heat of combustion of $H_2$ per mole of oxygen [13,14]. Methane conversion (Fig. 3b) also increased progressively, because of higher temperatures on the catalyst and higher partial pressures of water, that boosted the kinetically limited steam reforming reaction [9,11].
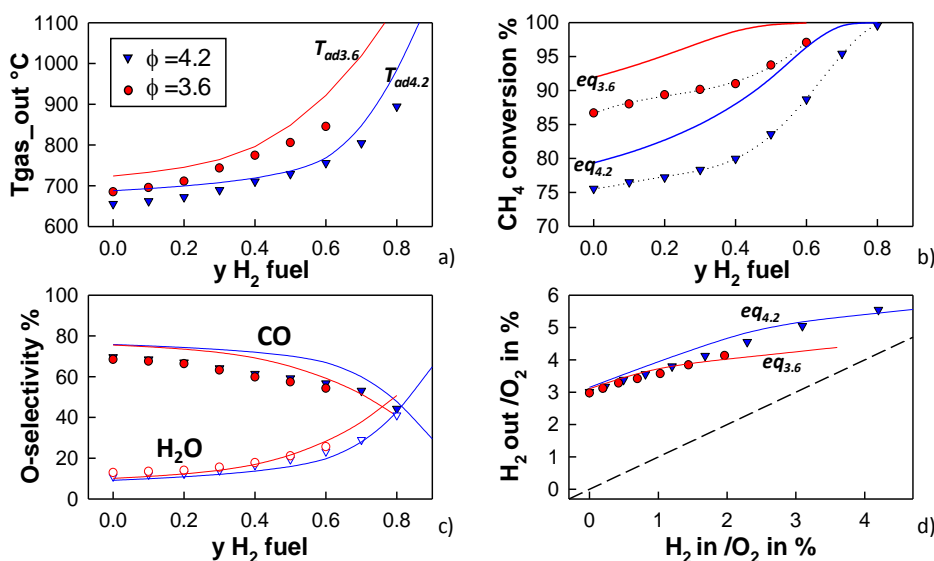


*Fig. 3. Effect of the $H_2$ content in $CH_4$-$H_2$ fuel blends during the CPO in air for two values of $\phi$ (3.6, 4.2) over Rh-Pt honeycomb monolith: a) temperature of gas leaving the catalyst, b) $CH_4$ conversion, and c) O-atom selectivity to CO and $H_2O$ as a function of $yH_2$; d) hydrogen production expressed as $H_2$ out /$O_2$ in vs. $H_2$ in /$O_2$ in. Solid lines represent thermodynamic equilibrium values (p, H=constant).*

The progressive substitution of $CH_4$ with $H_2$ shifted the process O-selectivity towards $H_2O$ rather than CO and $CO_2$ (Fig. 3c), with a distribution among the three oxygenated products which was rather unaffected by the specific level of $\phi$, and once again followed the equilibrium predictions. Figure 3d shows that the CPO reactor fuelled with $CH_4$-$H_2$ mixtures produced more hydrogen than it was fed under all the inlet conditions explored. By increasing the $H_2$ content in the fuel, the temperature peak progressively moved closer to the inlet section of the catalytic monolith: however we never observed a flashback. Therefore it can be argued that $H_2$ is rapidly and preferentially oxidized instead of the hydrocarbon in the first part of the catalytic reactor due to its higher reactivity and diffusivity, causing a marked increase of the catalyst temperature in this zone [13]. Further downstream the reactor $H_2$ is produced again via methane steam reforming [13].

The final composition of the syn-gas emerging from the CPO reactor at $\phi=4.2$ is shown in Fig. 4 as a function of the $H_2$ content in the fuel: the mole fraction of $H_2$ increased progressively from ca. 0.33 to 0.50, which was compensated by the drop in the concentration of CO (from 0.16 to 0.08) and $CH_4$ (from 0.05 to $3.7 \cdot 10^{-4}$); the overall concentration of diluents ($N_2$, $CO_2$ and $H_2O$) was slightly affected (0.42-0.46), but the water fraction increased.
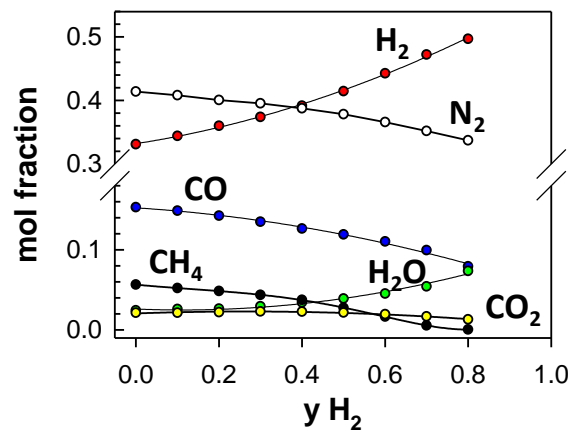


**Fig. 4.** *Composition of the syn-gas produced from the CPO in air of $CH_4$-$H_2$ blends at $\phi$ 4.2 over the Rh-Pt honeycomb monolith as a function of the $H_2$ content in the fuel.*

### 3.1. Combustion Performance of Hybrid Radiant Burner

In the hybrid burner, the catalytic stage prepares a hot syn-gas which is the actual fuel for the following homogeneous (flame) combustion stage. IR analysis of the hybrid burner (Figure 5) showed the presence of an axial-symmetric laminar diffusive flame structure surrounding the hot radiating catalytic reactor. The reactor presents a very uniform temperature distribution on the whole outer surface. The flame itself, which appeared blue in the visible range had a low-luminosity (typical of a premixed flame). No soot formation was found by Planar Laser Induced Incandescence, and this was confirmed by careful inspection of IR images collected at F=3.9 µm in the gas phase surrounding the burner (Fig.5 b).

Hot gas leaving the combustion head through the catalytic gauze were slightly colder than the catalyst itself. This was also confirmed by the thermocouple measurements [5] and implies that, inside the structured catalytic layer, heat generation occurs through surface oxidation reactions and the flowing gases are only heated by convection. Moving away from the catalytic surface along the radial coordinate we initially observed a flat temperature profile in the gas phase due to the absence of oxidation reactions close to the head: all of the oxygen from primary air was consumed by catalytic oxidation reactions (see next section), and more $O_2$ from the surrounding air had to diffuse to complete combustion. Thereafter, the gas temperature raised to a maximum in correspondence of a symmetric laminar diffusion flame front developed around the burner and above it, which was well captured by filtered profiles (F=4.25 µm). However, It should be underlined that temperature profiles in the gas phase were obtained by measuring the main emission peak of $CO_2$ at $\lambda$= 4.25 µm. These measurements are only qualitative due to the variation of the $CO_2$ concentration, the spatial integration of the emission, the flame thickness, the presence of an emitting/adsorbing/reflecting surface behind the flame [10] (which was particularly evident for low values of $\phi$, i.e. when the catalyst ran hotter). It is worth to note that this qualitative measurement is quite in a good agreement with temperature measurements operated with thermocouple.

The laminar flame envelope expanded at higher input power (and lower $\phi$), due to the corresponding higher flow rate and exit velocity of the gas leaving the catalytic head in the radial direction, which pushed the diffusive flame front away from the catalyst. It is also clear that the flame front extended well above the catalytic head, due to the relatively slow diffusion of oxygen from the surroundings and to poor mixing effectiveness with secondary air achieved by natural convection.
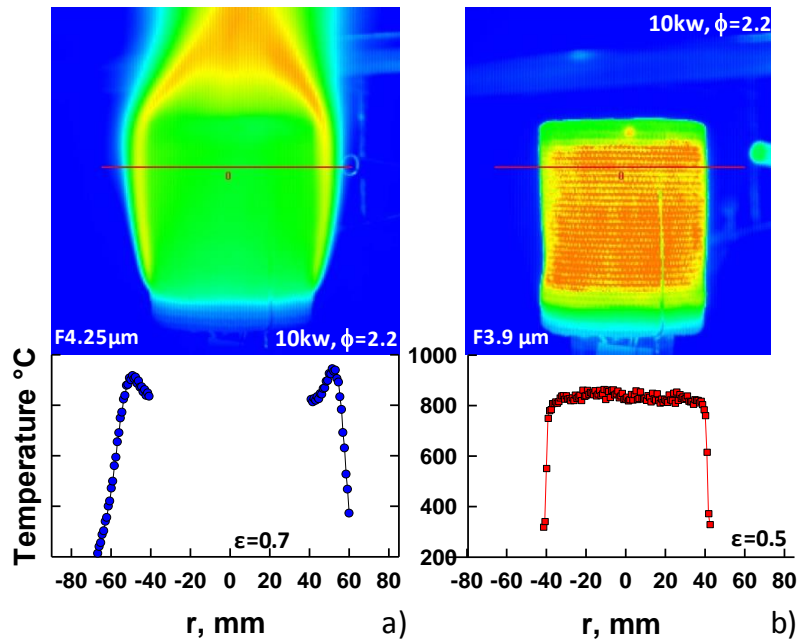
***Fig. 5.*** *InfraRed images of the flame structure ($CO_2$) and of the catalytic surface collected at 4.25µm (a) and 3.9µm (b) respectively, together with the corresponding temperature profiles at fixed height along the line shown in figure. Hybrid burner operated with pure methane at $\phi$=2.2, P=9.6kW*

Figure 6 shows that the flame structure and appearance did not change significantly by increasing the $H_2$ content of the fuel, while operating the burner at constant input power and equivalence ratio. This result can be easily rationalized by recalling the low dependency of the composition of the syn-gas produced in the CPO reactor with respect to large variations in the hydrogen content of the $CH_4$-$H_2$ fuel mixture (Fig. 4).

In line with our lab-scale CPO results, the temperature of the outer surface of the catalytic gauze increased progressively for lower values of $\phi$ and for higher $H_2$ contents in the fuel fed to the hybrid burner (Figure 6 and 7). The thermal resistance of the catalyst (i.e. its maximum allowable surface temperature) set the minimum permissible value $\phi$, which in turn depended on how much heat was removed from the radiating catalytic head [5,6].
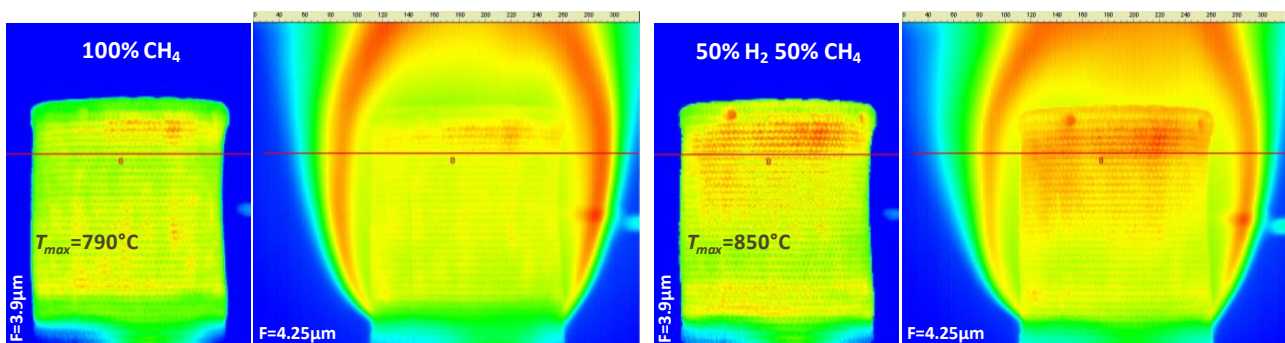


***Fig. 6.*** *InfraRed images of the catalytic surface and of the flame structure ($CO_2$) filtered at 3.9µm and 4.25µm respectively, during operation at $\phi$=3.6 and P=19.2kW with pure methane (left) and with a 50%$H_2$ - 50% $CH_4$ mixture (right). Surface temperature estimated with a solid emissivity ε=0.5 at 3.9µm.*

Figure 7 demonstrates that fuel blends very rich in $H_2$ were safely handled with the hybrid catalytic burner by increasing the feed equivalence ratio, in order to compensate the increase in the temperature level of the catalyst. At the same time larger values $\phi$ effectively contrasted the tendency of the highly reactive fuel to give a flashback in the mixing zone upstream of the catalyst, and indeed this was never observed even at the highest hydrogen contents.

Gas analysis at the exit of the catalytic partial oxidation stage invariably showed no trace of nitrogen oxides. Thus, $NO_x$ formation occurred only in the homogeneous flame combustion stage: in the simple current configuration of the hybrid burner, syn-gases emerging from the catalytic gauze were burned under purely diffusive and laminar conditions. The contribution from the thermal-$NO_x$ mechanism was strongly limited due to the significant reduction of the peak flame

temperature obtained by the interstage heat removal from the hot catalyst [6,16] independently from the type of the fuel and its $H_2$ content. This is clearly shown in Figure 7 where NO emissions appear to decrease for lower values of the feed equivalence ratio, which in turn correspond to higher surface temperatures and therefore to a larger amount of heat exchanged by radiation which bypassed the flame. In general it was found that the presence of up to 50% $H_2$ by volume in the fuel mixture did not alter the NO emission performance of the hybrid burner with respect to operation with pure $CH_4$ (Figure 7b), in line with the small variations in the composition of the syngas fuel and in the temperature of the radiating catalytic surface (Figure 7a). A slight increase in the total NO formation was observed for higher values of the $H_2$ content in the fuel, probably related to the corresponding increase in the peak flame temperature achieved in the secondary flame. As an example, the hybrid burner showed an outstanding NO emission level of 42 ppm (@0%$O_2$) when fuelled with a 80% $H_2$-$CH_4$ mixture at $\phi$=3.6 (P=9.6 kW), in comparison to the 33ppm measured with pure methane. It should be remarked that the prompt $NO_x$ formation mechanism in the syn-gas diffusion flame was progressively suppressed with increasing $yH_2$ in the fuel by two simultaneous factors: i) the decreasing concentration of (un-reacted) methane and CO in the syn-gas ; ii) its larger dilution by $H_2O$ [15,16]. Combustion tests run at different power levels for a fixed value of $\phi$ revealed that NO emissions increased slightly when the burner was operated at higher power, according to a proportionally lower fraction of the total heat of combustion which was transferred from the radiating element [5,6]. At the same time it was confirmed that up to 50% vol. of $H_2$ in the fuel had only a minor impact on the formation of nitrogen oxides.

The high preheating of the syn-gas fuel, as well as its large $H_2$ content, facilitated the oxidation of other organic fuel fractions (CO and residual $CH_4$) even in a secondary flame with poor mixing judged by the standard of conventional design [16]. In agreement with our previous results [6], methane emissions in the exhaust were always below the detection limit (10ppm) regardless of the $H_2$ content in the fuel mix. CO emissions were always ≤ 40ppm (corrected @0% $O_2$), and decreased progressively when increasing $yH_2$ in the fuel and the input power to the burner.
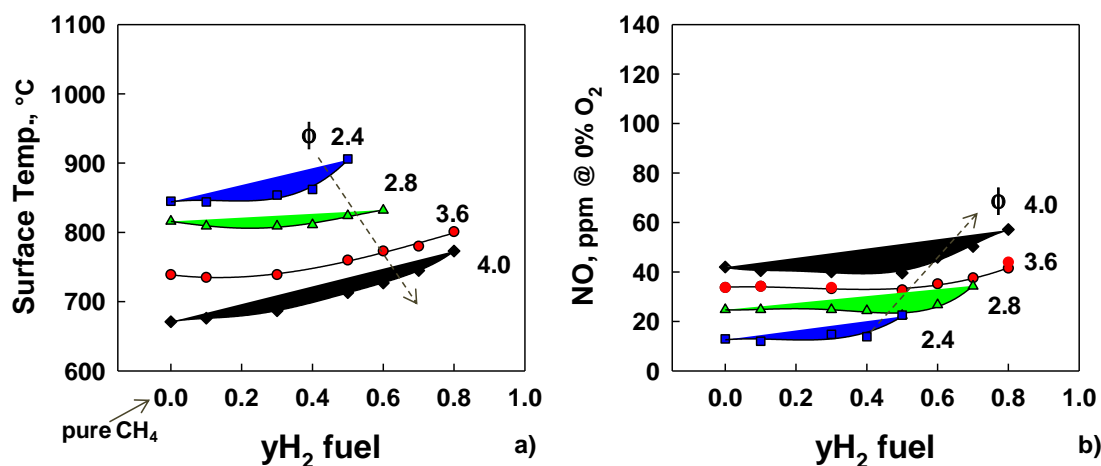


**Fig. 7.** *a) Maximum temperature of the outer catalytic surface and b) NO emissions in the exhaust from the hybrid burner as a function of $H_2$ content in the $CH_4$-$H_2$ fuel mixture for several levels of $\phi$ at fixed input power (9.6 kW).*

## 4. Conclusions

The Catalytic Partial Oxidation of methane-hydrogen mixtures, intended as the first stage of conversion in a hybrid combustion system, was tested over Pt-Rh based structured reactors operated under self sustained high temperature conditions at short contact time. The progressive substitution of methane with $H_2$ in the fuel at fixed equivalence ratio induced an increase in the temperature level of the catalyst and in the conversion of methane to syn-gas, resulting in a net hydrogen production across the CPO reactor for all conditions explored. It is argued that $H_2$ was rapidly and preferentially oxidized instead of the hydrocarbon in the first part of the catalytic reactor due to its higher reactivity and diffusivity; further downstream $H_2$ was produced again via methane steam reforming.

A prototype radiant hybrid burner was safely operated at atmospheric pressure with up to 80% by volume of $H_2$ in the fuel and a primary equivalence ratio $\phi$ in the range 2.4 – 4.0. Outstandingly low-$NO_x$ emission levels were attained with a purely diffusive laminar flame combustion stage, due to an effective suppression of both thermal and prompt $NO_x$ formation mechanisms. In particular it was found that the presence of up to 50% $H_2$ in the fuel mixture did not alter the $NO_x$ emissions of the hybrid burner with respect to operation with pure $CH_4$, according to the small variations measured in the composition of the syn-gas burned in the secondary flame and to the slight increase in the temperature of the radiating catalytic surface. The rather large values of the feed equivalence ratio to the burner prevented flashback in the mixing zone upstream of the catalyst even at the highest hydrogen contents in the fuel.

## 5. Acknowledgments

## REFERENCES

[1] Sepman A., Mokhov A., Levinsky H., "The effects of $H_2$ addition on NO formation in atmospheric-pressure, fuel-rich-premixed, burner-stabilized methane, ethane and propane flames", Int. J. Hydrogen Energ., vol. 36, pp. 4474-4481, 2011.

[2] www.naturalhy.net EC project "Preparing for the hydrogen economy by using the existing natural gas system as catalyst", Final Report 2010.

[3] Chiesa P., Lozza G., Mazzocchi L., "Using Hydrogen as Gas Turbine Fuel", J Eng Gas Turb Power, vol. 127, pp. 73-80, 2005.

[4] Bairda B., Etemad S., Karim H., Alavandi S., Pfefferle W.C., "Gas turbine engine test of RCL catalytic pilot for ultra-low NOx applications", Catal. Today vol. 155, pp.13-17, 2010.

[5] Cimino S., Russo G., C. Accordini, G. Toniato, "Development of a hybrid catalytic burner", Combust. Sci. Tech., vol. 182, pp. 380-391, 2010.

[6] Cimino S., Allouis C., Pagliara R., Russo G., "Effect of catalyst formulation on the performance of a natural gas hybrid catalytic burner", Catal. Today, vol. 171, pp. 72-78, 2011.

[7] Panuccio G, Dreyer B, Schmidt LD. A Comparison of the Catalytic Partial Oxidation of C1 to C16 Normal Paraffins. AIChE Journal, vol. 53, pp. 187-195, 2007.

[8] Deluga G, Salge J, Schmidt LD, Verykios X. Renewable Hydrogen from Ethanol by Autothermal Reforming. Science, vol. 303, pp. 993-997, 2004.

[9] Cimino S., Lisi L., Russo G., Torbati R., "Effect of partial substitution of Rh catalysts with Pt or Pd during the partial oxidation of methane in the presence of sulphur", Catal Today, vol. 154, pp. 283-292, 2010.

[10] Brahmi L., Vietoris T., Torero J. L., Joulain P., "Estimation of boundary layer diffusion flame temperatures by means of an infrared camera under microgravity conditions", Meas. Sci. Technol., vol. 10, pp. 859–865, 1999.

[11] Horn R., Williams K.A., Degenstein N.J., Bitsch-Larsen A., Dalle Nogare D., Tupy S.A., Schmidt L.D., "Methane catalytic partial oxidation on autothermal Rh and Pt foam catalysts: oxidation and reforming zones, transport effects, and approach to thermodynamic equilibrium", J. Catal., vol. 249, pp. 380-393, 2007.

[12] Beretta A, Groppi G, Lualdi M, Tavazzi I, Forzatti P. Experimental and modelling analysis of methane partial oxidation: transient and steady state behavior of Rh-coated honeycomb monoliths", Ind. Eng. Chem. Res., vol. 48, pp. 3825-3836, 2009.

[13] Michael B.C., Nare D.N., Schmidt L.D., „Catalytic partial oxidation of ethane to ethylene and syngas over Rh and Pt coated monoliths: Spatial profiles of temperature and composition" Chem. Eng. Sci., vol. 65, pp. 3893-3902, 2010.

[14] Cimino S., Donsì F., Russo G., Sanfilippo D., "Olefins production by catalytic partial oxidation of ethane and propane over Pt/LaMnO3 catalyst", Catal Today, vol. 157, pp. 310-314, 2010.

[15] K. J. Whitty, H. R. Zhang, E. G. Eddings, "Emissions from Syngas Combustion" Combust. Sci. Tech., vol. 180, pp. 1117-1136, 2008.

[16] Giles D., Som S., Aggarwal S.,"NOx emission characteristics of counter-flow syngas diffusion flames with airstream dilution", Fuel, vol. 85, pp. 1729-1742, 2006.